NASA Technical Paper 2941

1989

Application of Newton's Method to Postbuckling of Rings Under Pressure Loadings

Gaylen A. Thurston
Langley Research Center
Hampton, Virginia

NASA
National Aeronautics and Space Administration
Office of Management
Scientific and Technical Information Division

Summary

The postbuckling response of circular rings (or long cylinders) is examined. The rings are subjected to four types of external pressure loadings; each type of pressure is defined by its magnitude and direction at points on the buckled ring. Newton's method is applied to the nonlinear differential equations of the exact inextensional theory for the ring problem. A zeroth approximation for the solution of the nonlinear equations, based on the mode shape corresponding to the first buckling pressure, is derived in closed form for each of the four types of pressure. The zeroth approximation is used to start the iteration cycle in Newton's method to compute numerical solutions of the nonlinear equations. The zeroth approximations for the postbuckling pressure-deflection curves are compared with the converged solutions from Newton's method and with similar results reported in the literature.

Introduction

The postbuckling behavior of circular rings (or of long cylinders) under external pressure is examined in this paper. The behavior is affected by the magnitude and direction of the pressure on the deformed ring. Four types of pressure loadings are considered: hydrostatic, constant directional, constant radial, and inverse-square radial. Each type is clearly defined in the paper in terms of the differential geometry of the deformed ring.

The ring is modeled by exact inextensional shell theory. Newton's method (ref. 1) is used to solve the nonlinear differential equations of the inextensional theory. Newton's method leads directly to the classical linear buckling problem that determines the buckling pressures and their corresponding eigenfunctions. Next, by specifying the amplitude of the first eigenfunction, a zeroth approximation is provided to start the iteration in Newton's method for the postbuckling solutions. A part of the zeroth approximation is to determine the pressure as a function of this amplitude by making the residual error in the zeroth approximation orthogonal to the first eigenfunction. This choice for the zeroth approximation in Newton's method is essentially the same as the method of averaging, which is well-known in nonlinear vibration theory. Newton's method is then used to correct the analytical zeroth approximation by a numerical solution of the linear variational equations of Newton's method. The numerical solution uses numerical harmonic analysis to compute Fourier series solutions for the ring postbuckling deflections as a function of angular position on the undeformed ring. The accuracy of the numerical solution is nearly exact, since it is limited only by truncating the Fourier series and by small round-off errors.

The theoretical results for the postbuckling of the ring are affected by terms in the theory that are often dropped in approximate nonlinear shell theory. Numerical results from inextensional theory are tabulated in the paper and compared with published results (refs. 2 through 10).

The zeroth approximation from Newton's method is compared with the numerical results for each type of pressure loading and proves to be a good approximation of the initial postbuckling behavior. The leading terms of the zeroth approximation are also compared with similar results in the literature derived from perturbation theory (refs. 2 through 6). The accuracy of the two approximations is comparable, but the analysis and algebraic operations for the zeroth approximation in Newton's method are more direct than the analysis in the perturbation method for the ring problem. The direct calculation reduces the chance for algebraic errors that can go undetected in a perturbation analysis.

Symbols

A, C, D	constants of integration in eigenfunction solution that depend on modal amplitude B
a	radius to point on undeformed circular ring
B	modal amplitude that appears as parameter in zeroth approximation, see equation (12)
EI	bending stiffness of ring cross section
is	pure imaginary exponent appearing in eigenfunction

$J_n(B)$	Bessel functions of first kind and order n
M, N, Q	stress resultants acting on cross-sectional area of ring
n	nondimensional stress resultant, Na^2/EI
P_t, P_n	tangential and normal pressure, respectively, force/unit of arc length
p_t, p_n	nondimensional components of pressure loading on deformed ring
q	pressure magnitude, force/unit of arc length
r	magnitude of position vector $\mathbf{r}$
$\mathbf{r}$	position vector for point on deformed ring
s	arc length of reference surface of ring
$\mathbf{t}, \mathbf{n}, \mathbf{e}_r, \mathbf{e}_\theta, \mathbf{i}, \mathbf{j}$	unit vectors
$\mathbf{U}$	vector function that is solution of nonlinear differential equations of inextensional theory for circular ring
$\delta\mathbf{U}$	vector function that is correction of $\mathbf{U}$ in Newton's method
V, W	magnitude of components of displacement vector, length
v, w	nondimensional displacements, $v = V/a$ and $w = W/a$
$\lvert w\rvert_{\max}$	maximum absolute value of w as function of θ
w_1	coefficient of $\cos 2\theta$ in Fourier series solution for w; parameter in results from perturbation theory
β	angle between position vector of point on deformed ring and corresponding vector for undeformed ring
θ	angle in cylindrical coordinates locating point on undeformed ring; independent variable in ring equations
λ	nondimensional load parameter, qa^3/EI
ρ	nondimensional variable, r/a
ϕ	angle between tangent vector at point on deformed ring and corresponding vector on undeformed ring
ϕ_1	coefficient of $\sin 2\theta$ in Fourier series solution for ϕ
Subscripts:	
H, R, C, S	type of pressure loading: hydrostatic, constant directional, constant radial, and inverse-square radial, respectively
j	dummy subscript in Fourier series solutions
m	mth iteration cycle in Newton's method

Primes with symbols indicate derivatives with respect to independent variable θ. Superscript T indicates a transposed matrix.

Geometric Relations for Types of Pressure Loadings

The four types of pressure loadings considered in this paper for the ring, or for a long cylinder neglecting end effects, are defined in terms of the differential geometry of the deformed ring. The directions of the loadings acting at a point on the deformed ring are shown graphically in figure 1.

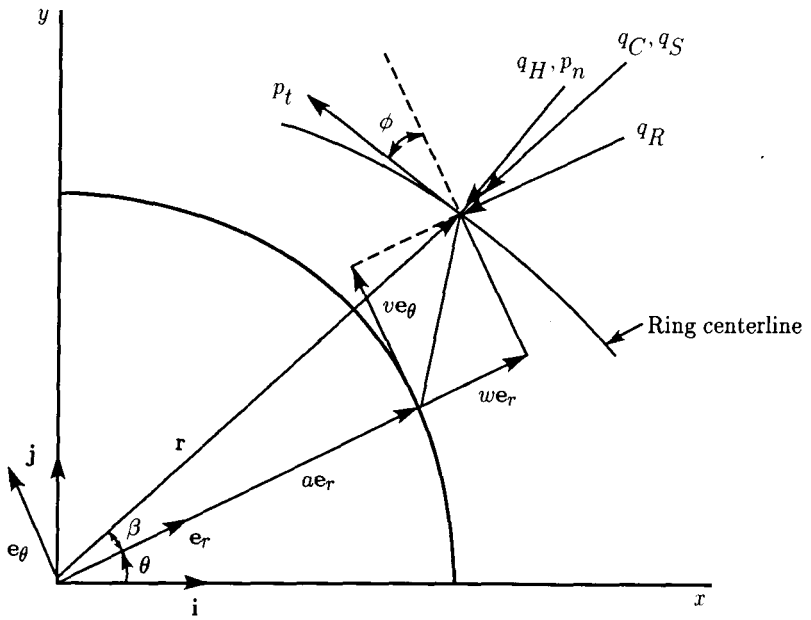

Figure 1. Pressure loadings applied to buckled ring.

The position vector for a point on the neutral surface of the undeformed ring is the usual vector for polar coordinates, as indicated in figure 1:

$$\mathbf{r} = a\mathbf{e}_r \tag{1}$$

where

$$\mathbf{e}_r = \cos\theta\ \mathbf{i} + \sin\theta\ \mathbf{j}$$

and $\mathbf{i}$ and $\mathbf{j}$ are unit vectors along the x- and y-axes. The constant directional pressure loading is constant in magnitude and acts in the direction opposite to the radial unit vector $\mathbf{e}_r$,

$$\mathbf{q}_R = -q_R\mathbf{e}_r \tag{2}$$

The dimensions of the magnitude q_R are force per unit of circumferential arc length. This pressure loading is normal to the undeformed ring, but does not necessarily remain normal at the corresponding point of application on the deformed ring.

The other three types of pressure loading are initially applied normal to the undeformed ring, but the direction is a function of the deflection of the ring. The direction of the two radial pressure loadings is defined by the position vector for a point on the neutral surface of the deformed ring as follows:

$$\mathbf{r} = (a + W)\mathbf{e}_r + V\mathbf{e}_\theta \tag{3}$$

where V and W are components of the displacement vector and $\mathbf{e}_\theta$ is the unit tangent vector for the undeformed ring. The constant magnitude radial pressure loading $\mathbf{q}_C$ acts in the opposite direction to the position vector $\mathbf{r}$.

The magnitude of the position vector is denoted by r,

$$r = (\mathbf{r}\cdot\mathbf{r})^{1/2} = \left[(a + W)^2 + V^2\right]^{1/2}$$

The unit vector for the position vector for the deformed shell makes an angle β with the position vector for the corresponding point on the undeformed shell,

$$\frac{\mathbf{r}}{r} = \cos\beta\ \mathbf{e}_r + \sin\beta\mathbf{e}_\theta = \frac{(a + W)\mathbf{e}_r + V\mathbf{e}_\theta}{r} \tag{4}$$

The constant radial pressure loading is defined by the relation

$$\mathbf{q}_C = -q_C(\cos\beta\ \mathbf{e}_r + \sin\beta\ \mathbf{e}_\theta) \tag{5}$$

The inverse square radial pressure loading is defined by the relation,

$$\mathbf{q}_S = -\frac{q_S a^2}{r^2}(\cos\beta\ \mathbf{e}_r + \sin\beta\ \mathbf{e}_\theta) \tag{6}$$

and is the only loading considered whose magnitude varies as a function of ring displacement.

The final pressure loading defined is hydrostatic pressure that acts normal to the deformed ring. The unit normal vector makes an angle ϕ with the undeformed position vector,

$$\mathbf{n} = -(\cos\phi\ \mathbf{e}_r + \sin\phi\ \mathbf{e}_\theta)$$

The hydrostatic pressure loading is defined by the following equation:

$$\mathbf{q}_H = q_H\mathbf{n} \tag{7}$$

The pressure loading terms appear in the nonlinear equilibrium equations for the ring or for the long cylinder. The notation for the stress resultants is shown in figure 2. The equilibrium equations are derived and nondimensionalized in appendix A.

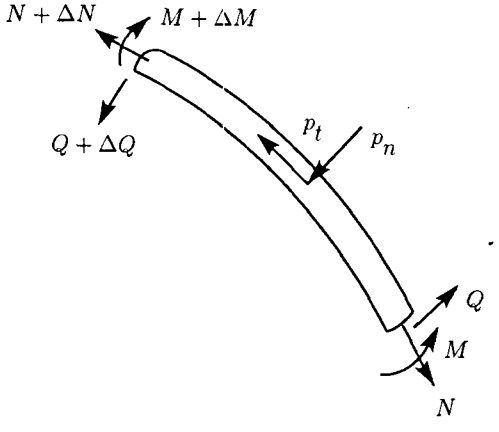

Figure 2. Stress resultants and pressures for buckled ring.

Newton's Method

The nondimensional equations derived in appendix A (eqs. (A15)) are a sixth-order set of ordinary equations in the nondimensional variables n, ϕ, v, and w. The independent variable is θ, the angle in polar coordinates that locates points on the undeformed ring. The set of nonlinear equations is solved herein by Newton's method following a general procedure outlined in reference 1. A solution of the equations where the ring remains circular can be written by inspection. This solution, the "membrane solution," becomes the zeroth approximation in Newton's method. A set of linear variational equations is derived in Newton's method by expanding nonlinear terms in the nonlinear differential equations about the zeroth approximation and retaining linear terms. Periodic solutions of the linear variational equations exist for certain critical values of the nondimensional load factors for the pressure loading. The first critical value for each separate loading corresponds to the "buckling pressure" from classical linear buckling theory.

After locating the critical load factors, Newton's method is continued to seek postbuckled solutions near the buckling pressure. The continuation consists of fixing a zeroth approximation for the postbuckled solution.

The zeroth approximation has a prescribed amplitude that multiplies the mode shape determined by the periodic solution of the linear variational equations derived from the membrane solution. The new zeroth approximation is used to derive a new sequence of linear variational equations. The sequence converges to the desired postbuckled solutions.

The convergence of the iteration for the postbuckled solution is improved by choosing a load factor in the new zeroth approximation that reduces the residual error in a least-squares sense. For the hydrostatic pressure case and the constant directional pressure case, the least-squares analysis can be carried out in closed form to give an approximate pressure-deflection relation. Similar accurate approximate results are obtained for the two radial pressure loadings, but the least-squares integrals cannot be evaluated in closed form. However, the integrals can be approximated by power series expansions or by numerical integration. The final results of the power series expansion are essentially the same as the results of the perturbation method reported in the literature (refs. 2 through 6); the difference in the two methods is the order of the mathematical operations.

Linear Variational Equations

The solution of the nonlinear differential equations is written as a vector function $\mathbf{U}$ in the following equation:

$$\mathbf{U}^T = [n,\ \phi,\ v,\ w] \tag{8}$$

Newton's method solves the nonlinear problem by solving the recursive sequence of linear problems, with iteration counter m, as

$$L(\mathbf{U}_{m-1})\delta\mathbf{U}_m = -E(U_{m-1}) \tag{9}$$

$$\mathbf{U}_m = \mathbf{U}_{m-1} + \delta\mathbf{U}_m \qquad (m = 1,\ 2,\ 3,\ \cdots) \tag{10}$$

For the nonlinear ring problem (eqs. (A15)), the linear variational equations (eq. (9)), are as follows:

$$\delta n'_m + (1 + \phi'_{m-1})\ \delta\phi''_m + \phi''_{m-1}\ \delta\phi'_m + \delta p_t = -(E_t)_{m-1} \tag{9a}$$

$$(1 + \phi'_{m-1})\ \delta n_m + n_{m-1}\ \delta\phi'_m - \delta\phi'''_m + \delta p_n = -(E_n)_{m-1} \tag{9b}$$

$$\delta w'_m - \delta v_m + \cos\phi_{m-1}\ \delta\phi_m = -(w' - v + \sin\phi)_{m-1} \tag{9c}$$

$$\delta w_m + \delta v'_m + \sin\phi_{m-1}\ \delta\phi_m = -(w + v' - \cos\phi)_{m-1} \tag{9d}$$

where

$$(E_t)_{m-1} = [n' + (1 + \phi')\phi'' + p_t]_{m-1}$$

$$(E_n)_{m-1} = [n(1 + \phi') - \phi''' + p_n]_{m-1}$$

$$\begin{aligned}\delta p_t = {} & [\lambda_R \cos\phi + (\lambda_C + \lambda_S\rho^{-2})\cos(\phi - \beta)]_{m-1}\ \delta\phi_m \\ & + [(\lambda_C + \lambda_S\rho^{-2})\rho^{-1}\sin\beta\cos(\phi - \beta) - 2\lambda_S\rho^{-3}\cos\beta\sin(\phi - \beta)]_{m-1}\ \delta w_m \\ & + [-(\lambda_C + \lambda_S\rho^{-2})\rho^{-1}\cos\beta\cos(\phi - \beta) - 2\lambda_S\rho^{-3}\sin\beta\sin(\phi - \beta)]_{m-1}\ \delta v_m\end{aligned}$$

$$\begin{aligned}\delta p_n = {} & -[\lambda_R \sin\phi + (\lambda_C + \lambda_S\rho^{-2})\sin(\phi - \beta)]_{m-1}\ \delta\phi_m \\ & - [(\lambda_C + \lambda_S\rho^{-2})\rho^{-1}\sin\beta\sin(\phi - \beta) + 2\lambda_S\rho^{-3}\cos\beta\cos(\phi - \beta)]_{m-1}\ \delta w_m \\ & + [(\lambda_C + \lambda_S\rho^{-2})\rho^{-1}\cos\beta\sin(\phi - \beta) - 2\lambda_S\rho^{-3}\sin\beta\cos(\phi - \beta)]_{m-1}\ \delta v_m\end{aligned}$$

All four nondimensional load parameters λ_H, λ_R, λ_C, and λ_S appear in the linear variational equations. In the numerical analysis, any combination of the four pressures can be applied. The results in this paper are restricted to the four cases of each pressure acting alone. The linear variational equations are derived by expanding nonlinear terms in the Taylor series in the variables n, ϕ, v, and w and retaining linear terms in the corrections δn, $\delta\phi$, δv, and δw. For example,

$$\cos\phi = \cos(\phi_{m-1} + \delta\phi_m) \approx \cos\phi_{m-1} - \sin\phi_{m-1}\ \delta\phi_m$$

$$\rho^{-1} \approx -\rho_{m-1}^{-1} - \rho_{m-1}^{-2}\ \delta\rho_m = -\rho_{m-1}^{-1} - \rho_{m-1}^{-3}\left[(1 + w_{m-1})\ \delta w_m + v_{m-1}\ \delta v_m\right]$$

Another useful relation in deriving the linear variational equations is the differential of the angle β,

$$d\beta = \frac{\cos\beta\ \delta v - \sin\beta\ \delta w}{\rho}$$

Membrane Solution and Buckling Pressures

Newton's method requires a zeroth approximation to start the iteration sequence. The expansion about zero,

$$\mathbf{U}_0^T = [0,\ 0,\ 0,\ 0]$$

gives the correction,

$$\delta\mathbf{U}_1 = [\delta n_1 = -\lambda_H - \lambda_R - \lambda_C - \lambda_S,\ 0,\ 0,\ 0]$$

and the converged solution, $\mathbf{U} = \delta\mathbf{U}_1$, the membrane solution. The next step is to determine if other solutions of the nonlinear equations exist in addition to the membrane solution. The analysis in Newton's method for identifying the existence of additional solutions consists of starting the usual iteration sequence with the known solution as the zeroth approximation. The linear variational equations in this case are homogeneous since the residual error of the known solution is zero. When the linear variational equations have nontrivial solutions that satisfy the boundary conditions, other solutions of the nonlinear problem exist. For the ring problem, the boundary conditions are that the solutions of the linear variational equations must be periodic in θ for certain critical values of the load parameters.

The solution of the linear homogeneous equations for the critical values of the pressure loadings is outlined in appendix B. The critical values of interest correspond to periodic solutions with two complete cycles around the ring, $s = 2$ in equations (B6):

$$\lambda_H = 3 \tag{11a}$$

$$\lambda_R = 4 \tag{11b}$$

$$\lambda_C = \frac{9}{2} \tag{11c}$$

$$\lambda_S = \frac{9}{4} \tag{11d}$$

Postbuckled Zeroth Approximation

The critical pressure load factor in each case is a bifurcation point marking the intersection of an additional solution with the membrane solution. To compute these additional solutions using Newton's method, it is necessary to start the iteration sequence with a new zeroth approximation that leads to a converged postbuckled solution. Selecting the new zeroth approximation for the ring problem proves to be a straightforward procedure. The analysis in appendix B determines eigenfunctions corresponding to each critical load. The eigenfunctions contain two arbitrary constants, and the zeroth approximation is determined by fixing these constants and adding the known function to the membrane solution. The new zeroth approximation results in a set of linear variational equations that no longer have periodic solutions for the homogeneous equations. On the other hand, the residual error on the right-hand side of the equations is periodic. Therefore, it is simple to show in theory that the particular solution of the equations is periodic and is a first correction for the zeroth approximation. An additional part of the analysis is to vary the load factor to keep the first correction small compared with the zeroth approximation. The choice of the load factor can be analytical or part of the numerical analysis of computing the first correction. The analytical choice will be considered first; the numerical analysis to determine the load factor is suggested by the analytical results.

The load factor is determined by making the residual error vector orthogonal to the eigenfunction in the zeroth approximation. For the ring problem, this orthogonalization can be written explicitly since the geometric

nonlinear terms are primarily functions of the angle ϕ. Therefore, guided by the form of the solutions with $s = 2$ in appendix B, let

$$\phi_0 = B \sin 2\theta \tag{12}$$

where B is now a prescribed constant rather than an arbitrary constant of integration and, as explained in appendix A and later in appendix B, an arbitrary phase angle in θ is ignored. Once ϕ_0 is known, it can be substituted for ϕ in the nonlinear equations. This substitution makes equations (A15c) and (A15d) linear equations in v and w. The particular solution of these equations for the zeroth approximation for v and w follows from the method of undetermined coefficients after making use of the expansions,

$$\sin \phi_0 = \sin(B \sin 2\theta) = 2 \sum_{k=1}^{\infty} J_{2k-1}(B) \sin(2k-1)\ 2\theta \tag{13a}$$

$$\cos \phi_0 = \cos(B \sin 2\theta) = J_0(B) + 2 \sum_{j=1}^{\infty} J_{2j}(B) \cos 4j\theta \tag{13b}$$

where $J_k(B)$ represents Bessel functions of the first kind and integer order:

$$w_0 = [-1 + J_0(B)] + \sum_{k=1}^{\infty} \frac{4(2k-1)}{(2k-1)^2 - 1} J_{2k-1}(B) \cos(2k-1)\ 2\theta$$

$$- \sum_{j=1}^{\infty} \frac{2}{16j^2 - 1} J_{2j}(B) \cos 4j\theta \tag{14a}$$

$$v_0 = \sum_{k=1}^{\infty} \frac{2}{(2k-1)^2 - 1} J_{2k-1}(B) \sin(2k-1)\ 2\theta$$

$$- 2 \sum_{j=1}^{\infty} \frac{8j}{16j^2 - 1} J_{2j}(B) \sin 4j\theta \tag{14b}$$

The integration of the first nonlinear equilibrium equation (eq. (A15a)) determines the zeroth approximation for the nondimensional stress resultant n as follows:

$$n_0 = c - \phi' - \frac{(\phi')^2}{2} - \int p_t\ d\theta \tag{15}$$

where c is a constant of integration to be determined and the zero subscript has been dropped on ϕ.

The only equation of the nonlinear equations not satisfied by the zeroth approximation is the equilibrium equation in the direction normal to the ring (eq. (A15b)). The residual error for the zeroth approximation for this equation is the result of substituting the expressions for ϕ_0 and for n_0, w_0, and v_0 into the equation. The general expression for the residual is

$$E_n = (1 + \phi') \left[c - \phi' - \frac{(\phi')^2}{2} \right] - \phi''' + \left[p_n - (1 + \phi') \int p_t\ d\theta \right] \tag{16}$$

The residual vanishes when ϕ is part of an exact solution. For the zeroth approximation $\phi_0 = B \sin 2\theta$, the residual is an even periodic function of θ and the fixed amplitude B. The constant of integration c and the pressure load factor λ for any given loading type are free parameters. They are determined by equating to zero the first two terms in the Fourier cosine series for E_n. Details of this orthogonalization procedure are contained in appendix C. The general form of the two equations that determine c and λ is

$$c - 3B^2 + \lambda a_0 = 0 \tag{17a}$$

$$B(2c + 6 - 3B^2) + \lambda a_1 = 0 \tag{17b}$$

where a_0 and a_1 are Fourier coefficients that depend on the type of pressure loading terms in the expressions for p_n and p_t and are functions of the modal amplitude B. Eliminating the constant c gives the load factor as a function of B:

$$\lambda = \frac{3(1 + B^2/2)}{a_0 - a_1/2B} \tag{18}$$

Equation (18) takes the following forms for the four load types:

1. Hydrostatic pressure:

$$\lambda_H = 3\left(1 + \frac{B^2}{2}\right) \tag{19a}$$

since $a_0 = 1$ and $a_1 = 0$ for this case.

2. Constant directional pressure:

$$\lambda_R = \frac{3(1 + B^2/2)}{J_0 + BJ_1(B) - J_1(B)/2B} \tag{19b}$$

which is derived from equation (13b) and the indefinite integral of equation (13a). For small values of B, the above equation is approximated by

$$\lambda_R \approx \frac{4(1 + B^2/2)}{1 + 3B^2/8} \approx 4\left(1 + \frac{B^2}{8}\right) \tag{19c}$$

3. Constant radial pressure:

The Fourier analysis in appendix C does not give a simple expression for equation (18) for this case. The approximate results for the Fourier coefficients are

$$a_0 = 2 \text{ and } \frac{a_1}{2B} = \frac{4}{3} - \frac{32}{135}B^2$$

so that equation (18) for constant radial pressure becomes

$$\lambda_C \approx \frac{3(1 + B^2/2)}{(2/3)\,(1 + 16B^2/45)} \approx \frac{9}{2}\left(1 + \frac{13B^2}{90}\right) \tag{19d}$$

4. Inverse-square radial pressure:

The approximate results for the Fourier coefficients from appendix C for this case are

$$a_0 = \left(\frac{8}{9}\right)B^2 \text{ and } \frac{a_1}{2B} = -\left(\frac{4}{3}\right) - \left(\frac{44}{45}\right)B^2$$

Equation (18) for inverse-square radial pressure is therefore

$$\lambda_S \approx \frac{3(1 + B^2/2)}{(4/3)(1 + 7B^2/5)} \approx \left(\frac{9}{4}\right)\left(1 - \frac{9B^2}{10}\right) \tag{19e}$$

This is the only loading with a negative coefficient for B^2 in the zeroth approximation for the postbuckling load; this implies that the ring is imperfection sensitive for an inverse-square radial pressure.

Fixing the load factors completely defines the four zeroth approximations for solutions for the postbuckled ring. All the dependent variables of the problem are periodic functions of the independent variable θ and contain the modal amplitude B as a parameter.

Iteration for Postbuckled Solutions

After determining the zeroth approximations, the residual error E_n (eq. (16)) in the solution of the normal equilibrium equation is an even periodic function that has the coefficient of $\cos 4\theta$ as the leading coefficient in its Fourier series. The residual error can be reduced to zero as part of the usual iteration in Newton's method that corrects the zeroth approximation. The iterative procedure cannot be carried out in closed form, but the insight gained in the analysis for the zeroth approximation makes clear the required properties of the numerical analysis. In fact, the algorithm is almost a direct numerical analog to the zeroth approximation. The linear variational equations for the ring (eqs. (9)) are solved for a periodic particular solution at each iteration step. For solutions at load factors near the critical values, the load factors are varied to keep these particular solutions for the corrections small.

The nontrivial zeroth approximation derived in the preceding section is corrected by the iteration sequence in equations (9) and (10). The iteration sequence starts with the iteration counter $m = 1$ and

$$\mathbf{U}_0^T = [n_0{=}n_0(B,\theta),\ \phi_0{=}B\sin 2\theta,\ v_0{=}v_0(B,\theta),\ w_0{=}w_0(B,\theta)]$$

The load factor for each case is also a function of the constant B as derived in the preceding section.

The linear variational equations (eqs. (9)) have variable coefficients and are solved numerically. The algorithm is a numerical analog to the zeroth approximation; the periodic zeroth approximation is corrected at each iteration step with a correction that is periodic with a least period of π in the independent variable θ. Formally, the iteration assumes that a periodic particular solution of the linear differential equations exists at each iteration step and that the corresponding homogeneous solutions can be ignored.

Floquet theory applies to the solution of differential equations with periodic coefficients. This theory suggests that the algorithm used here will converge. Lack of convergence would be an indicator that the solution of the homogeneous equations cannot be ignored. However, the iteration converges rapidly for the practical range of load factors considered in this paper.

The particular solution of the linear variational equations for the mth iteration step is sought in the form

$$[\delta\mathbf{U}]_m = \begin{bmatrix} \delta n_m \\ \delta\phi_m \\ \delta w_m \\ \delta v_m \end{bmatrix} = \begin{bmatrix} \sum_{j=0}^{J} n_{mj}\cos 2j\theta \\ \sum_{j=1}^{J} \phi_{mj}\sin 2j\theta \\ \sum_{j=0}^{J} w_{mj}\cos 2j\theta \\ \sum_{j=1}^{J} \phi_{mj}\sin 2j\theta \end{bmatrix} \qquad (m = 1, 2, 3, \cdots) \qquad (20)$$

The form of the particular solution continues the form of the zeroth approximation where ϕ and v are odd functions of θ and n and w are even functions. As discussed in appendixes A and B, the choice of even and odd periodic functions amounts to prescribing an arbitrary phase angle in the final periodic solution vector for the nonlinear system of equations. The series solutions are truncated to J terms with J as an input variable in the numerical solution. Substituting the assumed form of the particular solution (eqs. (20)) into the linear variational equations (eqs. (9)) and equating like coefficients of $\sin 2j\theta$ and $\cos 2j\theta$ result in $(4J + 2)$ linear algebraic equations in as many unknown Fourier coefficients. In the numerical solution, the periodic coefficients in the set of differential equations are expanded in a Fourier series by using numerical harmonic analysis. These series in turn multiply the assumed series solutions for the dependent variables and the series for their derivatives. The products of series are combined

into one series for each linear variational equation. The Fourier coefficients of the combined series are linear combinations of the undetermined coefficients in $\delta\mathbf{U}$ (eqs. (20)), and finally these coefficients of like trigonometric terms are equated to known coefficients computed by expanding the residual error on the right-hand sides of the linear variational equations by numerical harmonic analysis. The final numerical operation is to solve the resulting set of linear algebraic equations for the unknown Fourier coefficients in $\delta\mathbf{U}$. In summary, numerical harmonic analysis and trigonometric identities are used to implement a Galerkin solution.

When the parameter B in the zeroth approximation is small, the algebraic equations to determine the Fourier coefficients in the particular solution are nearly singular. When $B = 0$, the equations are singular since they coincide with similar singular equations in appendix B. To keep the correction at each iteration step as small as possible, the load factor λ is incremented in the residual error term for each type of pressure loading.

The matrix form of the linear algebraic equations for the mth iteration step is then

$$\mathbf{K}_{m-1}\mathbf{X}_m = -\mathbf{E}_{m-1} - \delta\lambda \left[\frac{\partial E}{\partial \lambda}\right]_{m-1} \qquad (m = 1, 2, 3, \cdots) \tag{21}$$

where $\mathbf{X}^T = [v_{mj},\ w_{mj},\ n_{mj},\ \phi_{mj}]$.

The algebraic equations (eq. (21)) are solved by a standard Gaussian elimination routine that factors the matrix $\mathbf{K}$ into an upper triangular form with pivoting about the maximum column element at each step of the factorization. The equations are factored so that the last diagonal element multiplies ϕ_{m1}, the correction on B, the coefficient of $\sin 2\theta$ in the series for ϕ. This last diagonal element can be small, on the order of B, but the indicated division by the element is not performed. Instead, the increment on the load factor $\delta\lambda$ is computed so that the corresponding element on the right-hand side of the factored equations is zero. This operation is the numerical analog to the analysis in the zeroth approximation where B is fixed and λ is determined as a function of B by an orthogonality relation (eq. (17b)).

For larger values of B at loads away from the critical loads, the matrix $\mathbf{K}$ is well-conditioned, so that λ can be fixed during the iteration and the value of B corrected during the iteration.

Results

Results for each type of pressure loading are presented in this section. For each case, the iteration to correct the zeroth approximation converged rapidly, including cases where the load factor λ was prescribed on the postbuckling curve. The zeroth approximation for the pressure-deflection curves proved to be close to the final results.

The results are also compared with other results in the literature. The zeroth approximations are compared with first approximations from perturbation theory. Also, the final results from the inextensional theory used herein are compared with results obtained by other theories. These latter results have significance in evaluating the accuracy of approximate shell theory for cylindrical shells under pressure loadings.

The convergent pressure-deflection results for the four types of pressure loadings are summarized by the curves in figure 3. The nondimensional load factor λ for each type of pressure loading is plotted as a function of the maximum radial deflection toward the center of the ring. Because of the sign convention, this deflection is denoted as $|w|_{\max}$, the maximum absolute value of w as a function of θ, and is determined by summing the Fourier series for w in the converged numerical solution.

A summary of the accuracy of each zeroth approximation is plotted in figure 4. The dashed curves are the zeroth approximations for each type of pressure loading λ as a function of the parameter B, the amplitude of the rotation ϕ of the tangent vector in the postbuckled ring. The solid curves are the corresponding results for the pressure λ as a function of $B = \phi_1$, the Fourier coefficient of $\sin 2\theta$ in the converged numerical solution for ϕ. This comparison of results in the curves gives a quantitative measure of the validity of the assumption used to derive the zeroth approximation—namely, that the final postbuckled solutions are dominated by the eigenfunction corresponding to the buckling pressure.

The accuracy of the zeroth approximation for the pressure-deflection relations suggests that design and optimization studies can be based on the zeroth approximation. Failure criteria can be based on stresses and strains in postbuckled rings or cylinders. The numerical solution shows that the zeroth approximation gives engineering accuracy for bending stresses and transverse shear stress resultants, but the terms in the Fourier series solutions with higher wave numbers affect the final numerical results for stresses more than the results for the deflections.

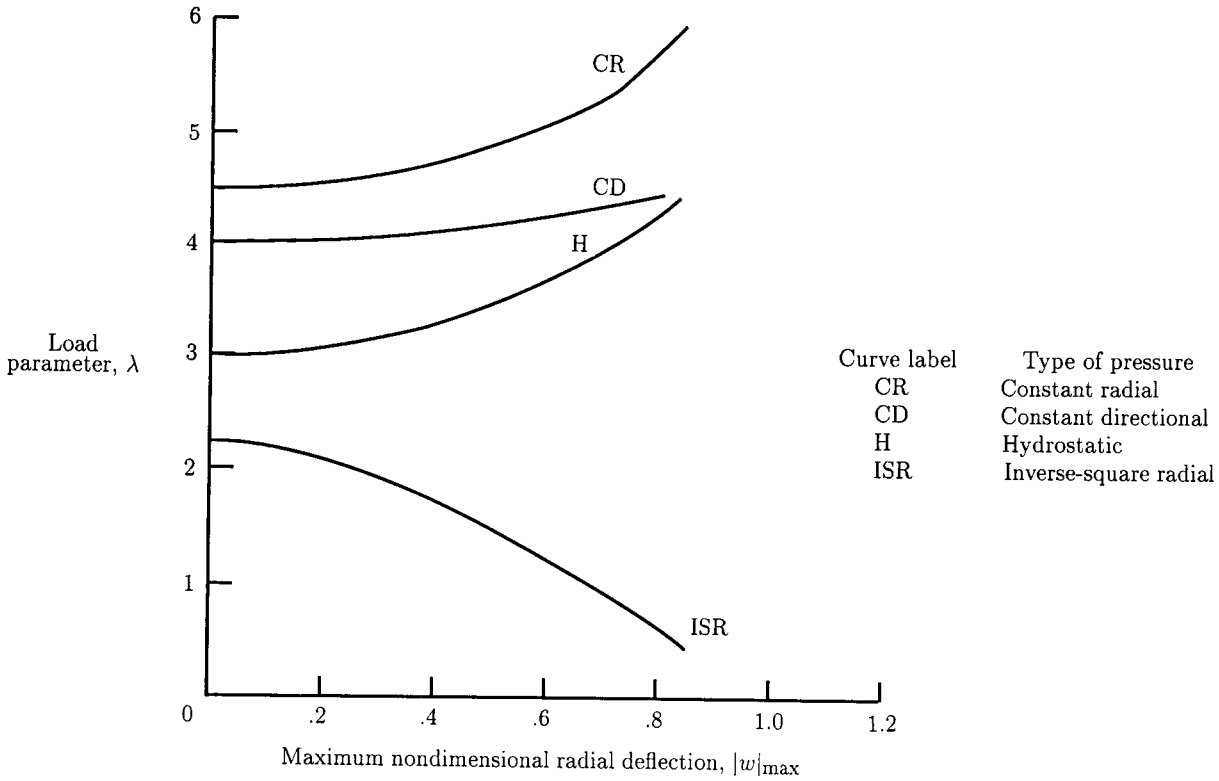

Figure 3. Nondimensional pressure versus maximum radial deflection.

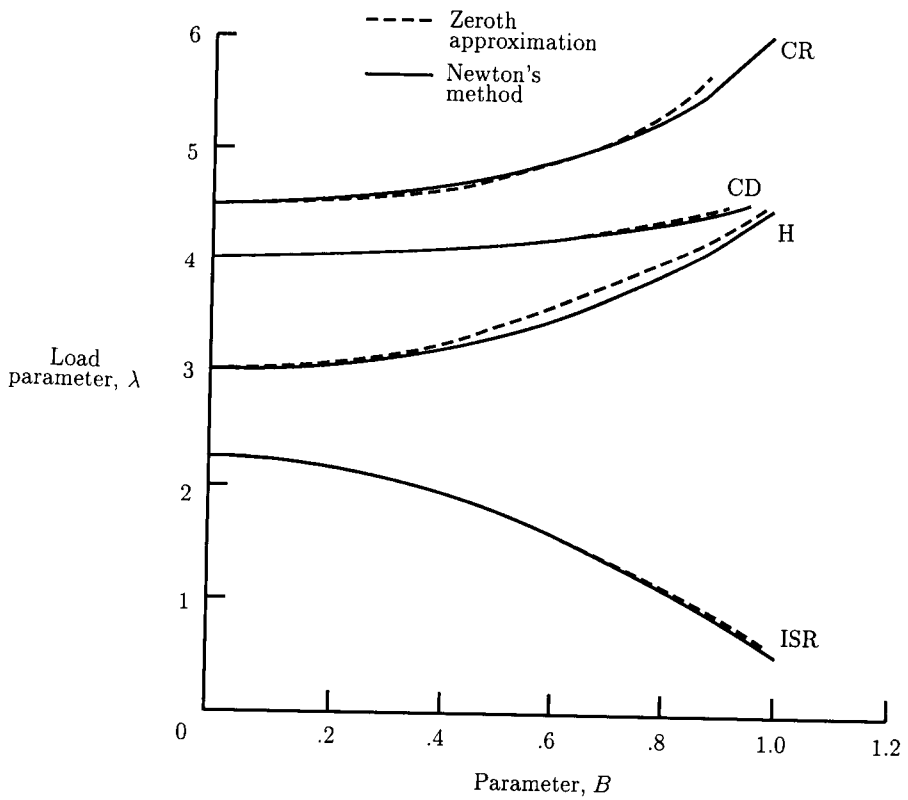

Figure 4. Zeroth approximation and converged solution from Newton's method.

Returning to the main results in this paper, postbuckled pressure-deflection relations, the results of the present analysis are compared with other results in the literature. Each case is considered separately in the following subsections.

Hydrostatic Pressure

Numerical results for this case are tabulated and compared with perturbation solutions given in table 1(a) and with an exact solution in table 1(b). The perturbation solution corresponds to the zeroth approximation, but a direct comparison of the two solutions is not possible. Formally, the solutions can be compared by equating the perturbation parameter w_1 to $2B/3$, the coefficient of $\cos 2\theta$ in the eigensolution for w in appendix B. However, it is more consistent in comparing the load factor from perturbation theory with the final load factor from Newton's method to set w_1 equal to the coefficient of $\cos 2\theta$ in the converged Fourier series for w. This latter choice for w_1 is used in computing all the tabulated results for the different pressure load factors from perturbation theory.

The perturbation approximation for the hydrostatic case from Sills and Budiansky (ref. 2), El Naschie and El Nashai (ref. 3), and Budiansky (ref. 4) is

$$\lambda_H = 3 + \frac{81}{32} w_1^2 \tag{22}$$

The perturbation expansion tabulated in table 1(a) for the hydrostatic pressure case is slightly closer to the numerical solution for the load factor than the corresponding zeroth approximation from Newton's method.

For the hydrostatic pressure case, the normal and tangential equilibrium equations are not coupled with the displacements, and equation (15) is a nonlinear differential equation in the derivative of ϕ. Because the independent variable θ does not appear explicitly in the equation, Carrier (ref. 5) was able to integrate the equation in closed form to give the load factor in terms of elliptic integrals. The results from Newton's method are compared with Carrier's results given in table 1(b). The load factors tabulated by Carrier are fixed input in Newton's method and the maximum derivative of ϕ as a function of θ is compared from the two solutions. The small discrepancies in the results are due to truncation and roundoff errors in calculating the two solutions.

An independent check of the numerical accuracy of the Galerkin solution used herein to solve the linear variational equations of Newton's method is available for the hydrostatic case. The tangential stress resultant N must balance the pressure times the deformed radius at points on the ring where the transverse shear vanishes. This check on Newton's method from statics shows at least an eight-digit accuracy for the results reported herein.

The theory used herein and in reference 5 is classified as an exact inextensional theory. Long cylinders under external pressure can also be modeled with nonlinear shell theory. Rehfield (ref. 6) reports a decrease in hydrostatic pressure with increasing deflection for a perturbation solution of Sanders' moderate bending theory (ref. 7). Hubka (ref. 8) checked Rehfield's results by using Newton's method. However, Hubka obtained pressure-deflection results closer to the inextensional theory by using a different approximate shell theory that accounts for the exact direction of the transverse shear stress resultant.

Comparison of different theoretical models for predicting postbuckling response of long cylinders under hydrostatic pressure is beyond the scope of the present paper. However, the results reported here show that the question of which shell theory will yield practical results for cylinders under hydrostatic pressure is not closed. The theoretical models should also include the capability to determine "imperfection sensitivity" of cylinders with imperfections in shape.

Constant Directional Pressure

The numerical results for constant directional pressure are listed in table 2. The definition of the deflection parameters is the same as for the hydrostatic pressure case. The zeroth approximation in equation (19b) is very good for this case, much better than the result from perturbation theory of El Naschie and El Nashai (ref. 3). Rehfield (ref. 6) reports that shell theory predicts neutral stability with the pressure remaining constant with displacement in the postbuckling range. Singer and Babcock (ref. 9) point out that constant directional pressure is unstable dynamically for complete rings that are not prevented from rotating about the axis of symmetry.

Constant Radial Pressure

Constant radial pressure results are summarized in table 3. The zeroth approximation from Newton's method (eq. (19c)) and the perturbation result of Sills and Budiansky (ref. 2)

$$\lambda_C = \frac{9}{2} + \frac{63}{32} w_1^2 \tag{23}$$

show comparable accuracy. However, the perturbation results of El Naschie and El Nashai (ref. 3) are not as accurate as the zeroth approximation.

Inverse-Square Radial Pressure

Results from radial pressure loading with the magnitude inversely proportional to the square of the radius are listed in table 4. This is the only loading that indicates imperfection sensitivity with postbuckled solutions at pressures below the critical bifurcation pressure. The zeroth approximation in equation (19d) is accurate, whereas the perturbation result of Sills and Budiansky (ref. 2)

$$\lambda_S = \frac{9}{4} - \frac{999}{112} w_1^2 \tag{24}$$

contains an algebraic error. The correct result (ref. 10) is

$$\lambda_S = \frac{9}{4} - \frac{999}{224} w_1^2 \tag{25}$$

One advantage of Newton's method for the ring problem is that the analysis in the zeroth approximation can be checked for errors by using numerical harmonic analysis to determine the Fourier coefficients a_0 and a_1 that depend on the type of loading. In turn, the numerical harmonic analysis is part of the computation in solving the linear variational equations to correct the zeroth approximations. If there are programming errors in computing the residual error at each step of the iteration, the iteration to correct the zeroth approximation will not converge. Therefore, although Newton's method is not foolproof, it is easier to detect errors in analysis or in computations than the perturbation method.

Concluding Remarks

The postbuckling behavior of complete rings and of long cylinders under external pressure depends on the direction of the pressure loads as well as on the magnitude of the pressure. For rings and long cylinders, nonlinear inextensional theory predicts different buckling pressures and different postbuckling behavior for four types of pressure loadings that are all directed toward the center of the ring when the pressure is initially applied. Hydrostatic pressure that is applied normal to the deformed ring and constant radial pressure have stable postbuckling equilibrium configurations. Constant directional pressure is also stable if rigid body rotation of the complete ring is suppressed by an external support. The postbuckled equilibrium states for radial pressure with a magnitude proportional to the inverse square of the deformed radius are unstable and exhibit imperfection sensitivity.

Newton's method provides both analytical and numerical results for the inextensional theory. Analytical results for a zeroth approximation in Newton's method compare favorably with perturbation results and can be derived more directly. Since much of the analysis can be written out explicitly, the ring problem is a good example of how the analysis in Newton's method can guide in the proper choice of algorithms for numerical solutions that are both efficient and reliable.

Results from inextensional theory presented herein and results reported in the literature from extensional shell theory with moderate rotations agree for the buckling pressures for long cylinders. The two theories show discrepancies in the postbuckling pressure-deflection curves for the case of hydrostatic pressure, the type of pressure usually found in engineering applications.

NASA Langley Research Center
Hampton, VA 23665-5225
July 28, 1989

Appendix A

Nonlinear Ring Equations

The equilibrium equations for the ring are derived in this appendix and then written in nondimensional form. The equilibrium equations are written by summing forces in the two directions normal and tangential to the deformed ring. The tangential direction is determined by differentiating the position vector $\mathbf{r}$ for the deformed ring

$$\mathbf{r} = (a + W)\mathbf{e}_r + V\mathbf{e}_\theta \tag{A1}$$

with respect to arc length s. The unit tangent vector, the result of the differentiation, is

$$\mathbf{t} = \left[\frac{dW}{ds} - V\,\frac{d\theta}{ds}\right]\mathbf{e}_r + \left[\frac{dV}{ds} + (a + W)\,\frac{d\theta}{ds}\right]\mathbf{e}_\theta \tag{A2}$$

The tangent vector of the deformed ring makes an angle ϕ with the tangent vector of the undeformed ring $\mathbf{e}_\theta$ so that, by definition,

$$\mathbf{t} = -\sin\phi\mathbf{e}_r + \cos\phi\mathbf{e}_\theta \tag{A3}$$

For any curve, the derivative of the unit tangent vector determines the curvature and its normal vector $\mathbf{n}$,

$$\frac{d\mathbf{t}}{ds} = \frac{1}{r_1}\mathbf{n} \tag{A4}$$

where $1/r_1$ is the curvature. The derivative of the tangent vector for the deformed ring (eq. (A3)) is

$$\frac{d\mathbf{t}}{ds} = -\left(\frac{d\phi}{ds} + \frac{d\theta}{ds}\right)(\cos\phi\mathbf{e}_r + \sin\phi\mathbf{e}_\theta) \tag{A5}$$

The theory outlined here is inextensional. The differential of arc length ds for the deformed ring is assumed to be the same as for the undeformed ring,

$$ds = a\,d\theta \tag{A6}$$

Therefore the curvature for the deformed ring in the inextensional theory is

$$\frac{d\phi}{ds} + \frac{d\theta}{ds} = \frac{1}{a}\frac{d\phi}{d\theta} + \frac{1}{a} \tag{A7}$$

The additional relation

$$\frac{d\mathbf{n}}{ds} = -\frac{1}{r_1}\mathbf{t} \tag{A8}$$

completes the geometric relations necessary to derive the equilibrium equations for the ring.

Equilibrium Equations

The stress resultants for the ring are shown in figure 2. Summing forces on a differential element of the deformed ring leads to the vector equation

$$\frac{d(N\mathbf{t})}{ds} + \frac{d(Q\mathbf{n})}{ds} + P_t\mathbf{t} + P_n\mathbf{n} = 0 \tag{A9}$$

where the tangential and normal components of the pressure loading are the projections of the pressure loadings defined earlier in the main text of the paper (also, see fig. 1):

$$P_t = q_R\sin\phi + \left(q_C + \frac{q_S a^2}{r^2}\right)\sin(\phi - \beta) \tag{A10a}$$

$$P_n = q_H + q_R\cos\phi + \left(q_C + \frac{q_S a^2}{r^2}\right)\cos(\phi - \beta) \tag{A10b}$$

The scalar components of the vector equilibrium equation are

$$\frac{dN}{ds} - \frac{1}{r_1} Q + P_t = 0 \tag{A11a}$$

$$\frac{1}{r_1} N + \frac{dQ}{ds} + P_n = 0 \tag{A11b}$$

The transverse shear force Q is eliminated by use of the moment equilibrium equation and the moment-curvature relation. The moment equilibrium equation is

$$\frac{dM}{ds} = Q \tag{A12}$$

It is assumed that the ring is thin so that the moment M is equal to the bending stiffness EI times the change in curvature of the ring.

$$M = -EI \left(\frac{1}{r_1} - \frac{1}{a} \right) = -EI \frac{d\phi}{ds} = -\frac{EI}{a} \frac{d\phi}{d\theta} \tag{A13}$$

Eliminating Q by using equation (A12) and then eliminating M by using equation (A13) give the equilibrium equations (A11) as

$$\frac{1}{a} \frac{dN}{d\theta} + \frac{EI}{a^3} \left(1 + \frac{d\phi}{d\theta} \right) \frac{d^2\phi}{d\theta^2} + P_t = 0 \tag{A14a}$$

$$\frac{1}{a} \left(1 + \frac{d\phi}{d\theta} \right) N - \frac{EI}{a^2} \frac{d^3\phi}{d\theta^3} + P_n = 0 \tag{A14b}$$

In addition to ϕ and θ, the pressure loading terms P_t and P_n are functions of the displacement components V and W. From the definition of the angle ϕ in the unit tangent vector $\mathbf{t}$ in equation (A2) and the expression for $\mathbf{t}$ in equation (A3),

$$\sin\phi = -\frac{1}{a} \left(\frac{dw}{d\theta} - V \right) \tag{A14c}$$

$$\cos\phi = 1 + \left(\frac{W}{a} + \frac{1}{a} \frac{dV}{d\theta} \right) \tag{A14d}$$

The set of differential equations (eqs. (A14)) contains four equations in the four dependent variables N, ϕ, V, and W in terms of the independent variable θ. Before solving the set of nonlinear differential equations, it is convenient to write them in nondimensional form.

Nondimensional Equations

Let the nondimensional variables be $w = W/a$, $v = V/a$, $n = Na^2/EI$, $\rho = r/a$, and $\lambda = qa^3/EI$. The nondimensional load parameters λ will be given the same subscript as the dimensional factors q. The nondimensional nonlinear differential equations corresponding to equations (A14) are

$$\frac{dn}{d\theta} + \left(1 + \frac{d\phi}{d\theta} \right) \frac{d^2\phi}{d\theta^2} + p_t = 0 \tag{A15a}$$

$$\left(1 + \frac{d\phi}{d\theta} \right) n - \frac{d^3\phi}{d\theta^3} + p_n = 0 \tag{A15b}$$

$$\frac{dw}{d\theta} - v + \sin\phi = 0 \tag{A15c}$$

$$1 + w + \frac{dv}{d\theta} - \cos\phi = 0 \tag{A15d}$$

$$p_t = \lambda_R \sin\phi + \left(\lambda_C + \lambda_S \rho^{-2}\right) \sin(\phi - \beta) \tag{A15e}$$

$$p_n = \lambda_R \cos\phi + \left(\lambda_C + \lambda_S \rho^{-2}\right) \cos(\phi - \beta) + \lambda_H \tag{A15f}$$

$$\rho^2 = (1 + w)^2 + v^2 \tag{A15g}$$

$$\cos\beta = \frac{1 + w}{\rho} \tag{A15h}$$

$$\sin\beta = \frac{v}{\rho} \tag{A15i}$$

The solutions of the nonlinear differential equations of physical interest are periodic in θ. If $\mathbf{U} = \mathbf{U}(\theta)$ is a solution, then $\mathbf{U}(\theta + \gamma)$ is also a solution where γ is any constant phase angle. The value of the phase angle is arbitrary; knowing that the phase angle exists helps guide the application of Newton's method by justifying the use of a sine series for certain functions in the numerical solutions and of a cosine series for other functions.

Appendix B

Linear Variational Equations for Zeroth Approximation

The linear homogeneous variational equations derived from the zeroth approximation,

$$\mathbf{U}_0^T = [n_0 = -\lambda_H - \lambda_C - \lambda_R - \lambda_S,\ 0,\ 0,\ 0] \tag{B1}$$

are the following:

$$\delta n_1' + \delta\phi_1'' + (\lambda_R + \lambda_C + \lambda_S)\,\delta\phi_1 - (\lambda_C + \lambda_S)\,\delta v_1 = 0 \tag{B2a}$$

$$\delta n_1 - (\lambda_H + \lambda_R + \lambda_C + \lambda_S)\,\delta\phi_1' - \delta\phi_1''' - 2\lambda_S\,\delta w_1 = 0 \tag{B2b}$$

$$\delta w_1' - \delta v_1 + \delta\phi_1 = 0 \tag{B2c}$$

$$\delta w_1 + \delta v_1' = 0 \tag{B2d}$$

The homogeneous equations have constant coefficients so that solutions can be sought in the exponential form,

$$\mathbf{U}_1^T = \left[Ae^{\sigma\theta},\ Be^{\sigma\theta},\ Ce^{\sigma\theta},\ De^{\sigma\theta}\right] \tag{B3}$$

For a nontrivial solution, the constants satisfy the relations,

$$C = -\sigma D$$

$$B = \left(\sigma^2 + 1\right) D$$

$$A = \left[\sigma\left(\sigma^2 + 1\right)\left(\sigma^2 + \lambda_H + \lambda_R + \lambda_C + \lambda_S\right) - 2\lambda_S\sigma\right] D$$

and the exponents are roots of the characteristic equation,

$$\sigma^2\left(\sigma^2 + 1\right)^2 + \sigma^2\left(\sigma^2 + 1\right)\lambda_H + \left(\sigma^2 + 1\right)^2\lambda_R + \sigma^2\left(\sigma^2 + 2\right)\lambda_C + \sigma^4\lambda_S = 0 \tag{B4}$$

The characteristic equation is cubic in σ^2 and can be solved in terms of the pressure load factors. However, for periodic solutions of the homogeneous linear variational equations, the characteristic exponents must be of the form

$$\sigma = \pm is \qquad \left(i^2 = -1;\ s = 0, 1, 2, 3, \cdots\right) \tag{B5}$$

Because of the condition that the solutions should be periodic, it is simpler to pick the characteristic exponents and solve the characteristic equation for the critical load factor. When each loading is treated separately, the critical load factors are

$$\lambda_H = \left(s^2 - 1\right) \tag{B6a}$$

$$\lambda_R = s^2 \tag{B6b}$$

$$\lambda_C = \frac{\left(s^2 - 1\right)^2}{s^2 - 2} \tag{B6c}$$

$$\lambda_S = \frac{\left(s^2 - 1\right)^2}{s^2} \tag{B6d}$$

The solutions of the differential equations for displacements corresponding to $s = 0$ and $s = 1$ are rigid body displacements and are not of physical interest, except for special cases where the ring has additional constraints. References 3 and 9 discuss this point for the case of λ_R, but the only solutions considered in the main text of this paper correspond to the exponents for $s = 2$.

The bifurcation points defined by $s = 2$ are all isolated. This suggests that Newton's method can be easily applied to computing solutions in the postbuckling range near the bifurcation points. The eigenfunctions corresponding to $s = 2$ have two arbitrary real constants when the exponential solutions with characteristic exponents $\sigma = \pm i2$ are put in real form. However, as noted at the end of appendix A, one of the two arbitrary constants is a phase angle in the periodic eigenfunctions. The other arbitrary constant is an amplitude of the periodic eigenfunctions and enters into the computation of solutions in the postbuckling range by Newton's method.

Appendix C

Fourier Analysis of Load Terms

This appendix contains the details of the computation of the Fourier analysis of the load terms. The load terms fix the load parameter as a step in determining the zeroth approximation to the postbuckled solution for the ring equations. In addition to the relations between the angles ϕ and β and the displacements v and w listed in the text of the paper, the two following relations are useful:

$$\sin(\phi - \beta) = -\rho' \tag{C1a}$$

$$\cos(\phi - \beta) = \rho + \frac{(1+w)v' - vw'}{\rho} \tag{C1b}$$

Using the relations in equations (C1), the load terms in equation (16) reduce to

$$\begin{aligned} p_n - (1+\phi') \int p_t \, d\theta = {} & \lambda_H + \lambda_R \left[\cos\phi - (1+\phi') \int \sin\phi \, d\theta \right] \\ & + \lambda_C \left[2\rho + \rho\phi' + \frac{(1+w)v' - vw'}{\rho} \right] \\ & + \lambda_S \left[\frac{(1+w)v' - vw'}{\rho^3} - \frac{\phi'}{\rho} \right] \end{aligned} \tag{C2}$$

When ϕ is a periodic function of the angle θ, the load terms are also periodic functions. The zeroth approximation for the load on the postbuckled ring is concerned with the two leading Fourier coefficients for each load term when $\phi = \phi_0 = B \sin 2\theta$. Squaring the zeroth approximation for $(1+w)$ and for v (eqs. (14)) and adding give

$$\begin{aligned} \rho^2 = (1+w)^2 + v^2 = {} & \left(J_0^2 + \frac{10}{9} J_1^2 + \frac{34}{225} J_2^2 + \cdots \right) \\ & + \left(\frac{8}{3} J_0 J_1 - \frac{8}{15} J_1 J_2 + \cdots \right) \cos 2\theta \\ & + \left(-\frac{4}{15} J_0 J_1 + \frac{2}{3} J_1^2 + \cdots \right) \cos 4\theta + \cdots \end{aligned} \tag{C3}$$

where the shorthand notation J_n is used for the Bessel functions $J_n(B)$. Similarly,

$$\begin{aligned} [(1+w)v' - vw'] = {} & \left(-\frac{16}{9} J_1^2 - \frac{64}{225} J_2^2 + \cdots \right) \\ & + \left(-\frac{4}{3} J_0 J_1 + \frac{12}{5} J_1 J_2 + \cdots \right) \cos 2\theta \\ & + \left(\frac{32}{15} J_0 J_2 + \cdots \right) \cos 4\theta + \cdots \end{aligned} \tag{C4}$$

The odd integer powers of ρ in the load terms are irrational functions of ρ^2. These functions can be represented by power series expansions, but the resulting expressions are lengthy. In computing the load parameter corresponding to the zeroth approximation, retaining up through cubic terms in the constant B, the amplitude of ϕ_0, provides a good approximation for continuing Newton's method to compute postbuckling solutions.

The MACSYMA program (ref. 11) for symbolic manipulations was used to generate the following truncated expressions:

$$\rho^m = 1 + \frac{mZ}{2} + \frac{m(m-2)Z^2}{8} + m(m-2)(m-4)Z^3 \qquad (m = 1,\ -1,\ -3) \tag{C5}$$

where $Z = \rho^2 - 1$ and

$$Z^2 = \left(\frac{32}{9}J_1^2\right) + \left(\frac{32}{3}A_0J_1 + \frac{208}{27}J_1^3 - \frac{32}{45}J_1J_2\right)\cos 2\theta + \left(\frac{32}{97}J_1^3\right)\cos 4\theta \tag{C6a}$$

$$Z^3 = \left(\frac{128}{9}J_1^3\right)\cos 2\theta \tag{C6b}$$

where $A_0 = J_0 - 1$. The expansion for the coefficient of the load factor λ_C is

$$2\rho + \rho\phi' + \frac{(1+w)v' - vw'}{\rho} = \left(2J_0 + \frac{4}{3}BJ_1 - \frac{14}{9}J_1^2 + \frac{8}{9}J_0J_1^2\right) + \left(2BJ_0 + \frac{8}{3}J_1 - \frac{4}{3}J_0J_1 + \frac{4}{3}A_0J_1J_2 + \frac{1}{9}BJ_1^2 + \frac{20}{9}J_1^3 - \frac{46}{27}J_0J_1^3 - \frac{2}{15}BJ_2 + \frac{92}{45}J_1J_2 - \frac{68}{45}J_0J_1J_2\right)\cos 2\theta \tag{C7a}$$

The leading terms in the power series that result from replacing the Bessel functions with their power series in their argument B are

$$2\rho + \rho\phi' + \frac{(1+w)v' - vw'}{\rho} = 2 + \left(\frac{8}{3}B - \frac{64}{135}B^3\right)\cos 2\theta \tag{C7b}$$

The expansion for the coefficient of the load factor λ_S follows the same steps,

$$\frac{(1+w)v' - vw'}{\rho^3} - \frac{\phi'}{\rho} = \left(\frac{4}{3}BJ_1 - \frac{16}{9}J_1^2 + \frac{16}{3}A_0J_1^2 + \frac{8}{3}J_0J_1^2\right) + \left(-2B + 2A_0B - \frac{4}{3}J_0J_1 + 4A_0J_1 - \frac{23}{9}BJ_1^2 + \frac{64}{9}J_1^3 - \frac{94}{9}J_0J_1^3 - \frac{2}{15}BJ_2 + \frac{12}{5}J_1J_2 - \frac{68}{15}J_0J_1J_2\right)\cos 2\theta \tag{C8a}$$

$$\frac{(1+w)v' - vw'}{\rho^3} - \frac{\phi'}{\rho} = \frac{8}{9}B^2 + \left(-\frac{8}{3}B - \frac{88}{45}B^3\right)\cos 2\theta \tag{C8b}$$

References

1. Thurston, G. A.: Continuation of Newton's Method Through Bifurcation Points. *J. Appl. Mech.*, vol. 36, no. 3, Sept. 1969, pp. 425–430.
2. Sills, L. B.; and Budiansky, B.: Postbuckling Ring Analysis. *J. Appl. Mech.*, vol. 45, no. 1, Mar. 1978, pp. 208–210.
3. El Naschie, M. S.; and El Nashai, Amr: Influence of Loading Behavior on the Post Buckling of Circular Rings. *AIAA J.*, vol. 14, no. 2, Feb. 1976, pp. 266–267.
4. Budiansky, Bernard: Theory of Buckling and Post-Buckling Behavior of Elastic Structures. *Advances in Applied Mechanics,* Volume 14, Chia-Shun Yih, ed., Academic Press, Inc., 1974, pp. 1–65.
5. Carrier, G. F.: On the Buckling of Elastic Rings. *J. Math. & Phys.*, vol. 26, 1947, pp. 94–103.
6. Rehfield, L. W.: Initial Postbuckling of Circular Rings Under Pressure Loads. *AIAA J.*, vol. 10, no. 10, Oct. 1972, pp. 1358–1359.
7. Sanders, J. Lyell, Jr.: Nonlinear Theories for Thin Shells. *Q. Appl. Math.*, vol. 21, no. 1, Apr. 1963, pp. 21–36.
8. Hubka, W. F.: Postbuckling Analysis of a Circular Ring Subjected to Hydrostatic Pressure. *J. Appl. Mech.*, vol. 40, no. 3, Sept. 1973, pp. 818–819.
9. Singer, J.; and Babcock, C. D.: On the Buckling of Rings Under Constant Directional and Centrally Directed Pressure. *J. Appl. Mech.*, vol. 37, no. 1, Mar. 1970, pp. 215–218.
10. Sills, L. B.: Erratum on Postbuckling Ring Analysis. *J. Appl. Mech.*, vol. 50, no. 3, Sept. 1983, p. 705.
11. *VAX UNIX MACSYMA*^{TM} *Reference Manual,* Version 11. Symbolics, Inc., c.1985.

Table 1. Summary of Different Results for Hydrostatic Pressure

(a) Nondimensional pressure-deflection results

Newton's method		Zeroth approximation		Perturbation theory	
λ_H	Deflection, $\lvert w\rvert_{\max}$	Rotation coefficient, $B = \phi_1$	$\lambda_H{}^a$	Deflection coefficient, w_1	$\lambda_H{}^b$
3.0	0	0	3.0	0	3.0
3.01128	.06910	.10	3.01500	.06659	3.01122
3.04543	.14279	.20	3.06000	.13275	3.04461
3.10346	.22063	.30	3.13500	.19804	3.09928
3.18710	.30214	.40	3.24	.26204	3.17381
3.30	.38758	.50085	3.37628	.32488	3.26717
3.40	.45019	.57275	3.49206	.36840	3.34354
3.44254	.47424	.60	3.54000	.38459	3.37440
3.62288	.56381	.70	3.73500	.44239	3.49539
3.84656	.65504	.80	3.96000	.49743	3.62632
4.00	.70866	.85816	4.10466	.52805	3.70581
4.12252	.74743	.90	4.21500	.54942	3.76409
4.20	.77035	.92468	4.28255	.56175	3.79877
4.40	.82467	.98304	4.44955	.59009	3.88140
4.46293	.84043	1.00000	4.50000	.59811	3.90552

$$^a\lambda_H = 3\left(1 + \frac{B^2}{2}\right).$$

$$^b\lambda_H = 3\left(1 + \frac{27w_1^2}{32}\right).$$

(b) Results for pressure versus maximum curvature change

		Maximum change of curvature, $\phi'(0)$, for–	
λ_H	Rotation coefficient, $B = \phi_1$	Newton's method	Elliptic integral solution
3.0	0	0	0
3.060	.22949	.47294	.475
3.227	.43883	.93239	.959
3.593	.68487	1.5175	1.53
4.076	.88454	2.0422	2.13
5.408	1.19941	3.0189	2.98

Table 2. Summary of Different Results for Constant Directional Pressure

Newton's method		Zeroth approximation[a]		Perturbation theory	
λ_R	Deflection, $\lvert w\rvert_{\max}$	Rotation coefficient, $B = \phi_1$	$\lambda_R{}^b$	Deflection coefficient, w_1	$\lambda_R{}^c$
4.0	0	0	4.0	0	4.0
4.0050	.06926	.1	4.00501	.06658	4.01995
4.02001	.14337	.2	4.02011	.13267	4.07921
4.04532	.22184	.3	4.04556	.19776	4.17599
4.10	.34118	.44377	4.10112	.28863	4.37488
4.12748	.38964	.5	4.12927	.32304	4.46960
4.18518	.47781	.6	4.18881	.38230	4.65769
4.25469	.56804	.7	4.26126	.43873	4.86618
4.33670	.65971	.8	4.34766	.49193	5.08898
4.40	.72251	.86796	4.41496	.52604	5.24523
4.50	.81106	.96349	4.52229	.57096	5.46698

[a]Tabulated values for λ_R for zeroth approximation are from equation (19b) rather than equation (19c).

[b]$\lambda_R = 4\left(1 + \frac{B^2}{8}\right)$.

[c]$\lambda_R = 4 + \frac{9w_1^2}{2}$.

Table 3. Summary of Different Results for Constant Radial Pressure

Newton's method		Zeroth approximation[a]		Perturbation theory	
λ_C	Deflection, $\lvert w\rvert_{\max}$	Rotation coefficient, $B = \phi_1$	$\lambda_C{}^b$	Deflection coefficient, w_1	$\lambda_C{}^c$
4.5	0	0	4.50	0	4.50
4.50878	.06936	.10	4.50657	.06658	4.50873
4.53545	.14377	.20	4.52717	.13261	4.53462
4.58109	.22269	.30	4.56447	.19757	4.57685
4.64771	.30555	.40	4.62312	.26091	4.63402
4.73863	.39176	.50	4.71021	.32211	4.70427
5.00	.56210	.68949	4.99615	.43035	4.86462
5.23452	.66427	.80	5.28623	.48762	4.96812
5.50	.74732	.88899	5.64187	.52990	5.05281
6.00	.84837	.99701	6.36480	.57569	5.15248

[a]Tabulated values for λ_C for zeroth approximation are from power series in Bessel functions generated by the MACSYMA code and are slightly different from values from equation (19d).

[b]$\lambda_C = \frac{9}{2}\left(1 + \frac{13B^2}{90}\right)$.

[c]$\lambda_C = \frac{9}{2} + \frac{63}{32}w_1^2$.

Table 4. Summary of Different Results for Inverse-Square Radial Pressure

Newton's method		Zeroth approximation[a]		Perturbation theory	
λ_S	Deflection, $\lvert w\rvert_{\max}$	Rotation coefficient, $B = \phi_1$	$\lambda_S{}^b$	Deflection coefficient, w_1	$\lambda_S{}^c$
2.25	0	0	2.25	0	2.25
2.24	.04870	.07105	2.23979	.04734	2.24
2.17113	.14350	.20	2.16969	.13265	2.17152
2.07370	.22213	.30	2.07117	.19771	2.07567
1.93944	.30464	.40	1.93656	.26125	1.94561
1.77048	.39048	.50	1.76884	.32281	1.78526
1.56947	.47909	.60	1.57136	.38192	1.59948
1.33960	.56989	.70	1.34770	.43817	1.39376
1.08445	.66233	.80	1.10133	.49116	1.17412
.80785	.75588	.90	.83519	.54055	.94687
.50	.85420	1.0044	.53799	.58799	.70810

[a]Tabulated values for λ_S for zeroth approximation are from power series in Bessel functions generated by the MACSYMA code and are slightly different from values from equation (19e).

[b]$\lambda_S \approx \frac{9}{4}\left(1 - \frac{9B^2}{10}\right)$.

[c]$\lambda_S = \frac{9}{4} + \frac{999}{224}w_1^2$.

NASA
National Aeronautics and Space Administration

Report Documentation Page

1. Report No.	2. Government Accession No.	3. Recipient's Catalog No.
NASA TP-2941		

4. Title and Subtitle	5. Report Date
Application of Newton's Method to Postbuckling of Rings Under Pressure Loadings	October 1989
	6. Performing Organization Code
7. Author(s)	8. Performing Organization Report No.
Gaylen A. Thurston	L-16578
9. Performing Organization Name and Address	10. Work Unit No.
NASA Langley Research Center Hampton, VA 23665-5225	505-63-01-09
	11. Contract or Grant No.
12. Sponsoring Agency Name and Address	13. Type of Report and Period Covered
National Aeronautics and Space Administration Washington, DC 20546-0001	Technical Paper
	14. Sponsoring Agency Code

15. Supplementary Notes

16. Abstract

The postbuckling response of circular rings (or long cylinders) is examined. The rings are subjected to four types of external pressure loadings; each type of pressure is defined by its magnitude and direction at points on the buckled ring. Newton's method is applied to the nonlinear differential equations of the exact inextensional theory for the ring problem. A zeroth approximation for the solution of the nonlinear equations, based on the mode shape corresponding to the first buckling pressure, is derived in closed form for each of the four types of pressure. The zeroth approximation is used to start the iteration cycle in Newton's method to compute numerical solutions of the nonlinear equations. The zeroth approximations for the postbuckling pressure-deflection curves are compared with the converged solutions from Newton's method and with similar results reported in the literature.

17. Key Words (Suggested by Authors(s))
Postbuckling
Rings
Long cylinders
Radial pressure
Hydrostatic pressure
Newton's method

18. Distribution Statement
Unclassified–Unlimited

Subject Category 39

19. Security Classif. (of this report)	20. Security Classif. (of this page)	21. No. of Pages	22. Price
Unclassified	Unclassified	25	A03